

The University of Akron
IdeaExchange@Uakron

Mechanical Engineering Faculty Research

Mechanical Engineering Department

7-1-2007

Investigation of the Stability of the Compressive Residual Stress Generated by Warm Laser Shock Peening

Chang Ye

University of Akron, Main campus

Please take a moment to share how this work helps you [through this survey](#). Your feedback will be important as we plan further development of our repository.

Follow this and additional works at: http://ideaexchange.uakron.edu/mechanical_ideas

Recommended Citation

Ye, Chang, "Investigation of the Stability of the Compressive Residual Stress Generated by Warm Laser Shock Peening" (2007). *Mechanical Engineering Faculty Research*. 775.

http://ideaexchange.uakron.edu/mechanical_ideas/775

This Dissertation is brought to you for free and open access by Mechanical Engineering Department at IdeaExchange@Uakron, the institutional repository of The University of Akron in Akron, Ohio, USA. It has been accepted for inclusion in Mechanical Engineering Faculty Research by an authorized administrator of IdeaExchange@Uakron. For more information, please contact mjon@uakron.edu, uapress@uakron.edu.

**PURDUE UNIVERSITY
GRADUATE SCHOOL
Thesis/Dissertation Acceptance**

This is to certify that the thesis/dissertation prepared

By Chang Ye

Entitled INVESTIGATION OF THE STABILITY OF THE COMPRESSIVE RESIDUAL STRESS
GENERATED BY WARM LASER SHOCK PEENING

For the degree of Doctor of Philosophy

Is approved by the final examining committee:

Gary J. Cheng Xianfan Xu
Chair

C. Richard Liu

Yung Shin

Eric A. Stach

To the best of my knowledge and as understood by the student in the *Research Integrity and Copyright Disclaimer (Graduate School Form 20)*, this thesis/dissertation adheres to the provisions of Purdue University's "Policy on Integrity in Research" and the use of copyrighted material.

Approved by Major Professor(s): Gary J. Cheng

Approved by: C. Richard Liu 07/01/2011
Head of the Graduate Program Date

**PURDUE UNIVERSITY
GRADUATE SCHOOL**

Research Integrity and Copyright Disclaimer

Title of Thesis/Dissertation:

INVESTIGATION OF THE STABILITY OF THE COMPRESSIVE RESIDUAL STRESS
GENERATED BY WARM LASER SHOCK PEENING

For the degree of Doctor of Philosophy

I certify that in the preparation of this thesis, I have observed the provisions of *Purdue University Executive Memorandum No. C-22*, September 6, 1991, *Policy on Integrity in Research*.*

Further, I certify that this work is free of plagiarism and all materials appearing in this thesis/dissertation have been properly quoted and attributed.

I certify that all copyrighted material incorporated into this thesis/dissertation is in compliance with the United States' copyright law and that I have received written permission from the copyright owners for my use of their work, which is beyond the scope of the law. I agree to indemnify and save harmless Purdue University from any and all claims that may be asserted or that may arise from any copyright violation.

Chang Ye

Printed Name and Signature of Candidate

07/01/2011

Date (month/day/year)

*Located at http://www.purdue.edu/policies/pages/teach_res_outreach/c_22.html

INVESTIGATION OF THE STABILITY OF THE COMPRESSIVE RESIDUAL
STRESS GENERATED BY WARM LASER SHOCK PEENING

A Dissertation
Submitted to the Faculty
of
Purdue University
by
Chang Ye

In Partial Fulfillment of the
Requirements for the Degree
of
Doctor of Philosophy

August 2011
Purdue University
West Lafayette, Indiana

UMINumber:3480932

Allrightsreserved

INFORMATIONTOALLUSERS

Thequalityofthisreproductionisdependentonthequalityofthecopysubmitted.

Intheunlikelyeventthattheauthoridnotsendacompletemanuscript
andtherearemissingpages,thesewillbenoted.Also,ifmaterialhadtoberemoved,
anotewillindicatethedeletion.



UMI3480932

Copyright2011byProQuestLLC.

Allrightsreserved.Thiseditionoftheworkisprotectedagainst
unauthorizedcopyingunderTitle17,UnitedStatesCode.



ProQuestLLC.
789EastEisenhowerParkway
P.O.Box1346
AnnArbor,MI48106-1346

To my parents, 叶远汉 胡多先

PREVIEW

ACKNOWLEDGMENTS

I would like to express my sincere gratitude to my advisor Dr. Gary J. Cheng for his insightful guidance that helped me achieve independence in research. I would also like to thank my committee members, Dr. Richard Liu, Dr. Yung Shin, Dr. Eric A. Stach and Dr. Xianfan Xu, for taking the time to serve as my committee members and give me valuable suggestions for my research.

I especially want to thank Dr. Eric A. Stach, Sergey Suslov, Patrick Cantwell, and Robert Colby from the School of Materials Engineering at Purdue University for their help with the TEM work. Dr. Jay Shi from Global Engineering & Materials, Inc. is acknowledged for granting us the permission to use the XFEM code.

Thanks also goes to all my labmates in the Bulk Micro Nano Manufacturing Laboratory at Purdue for their help and friendship inside and outside the lab. All the staff members, especially Wayne Ewbank, from the School of Industrial Engineering are acknowledged for their help and support.

I am deeply indebted to my parents for all the sacrifice they have made all these years. My greatest appreciation goes to my wife Lingli and my daughter Amber for their love. My thanks also goes to my sister Lei and my parents-in-law for their encouragement. Finally, I would like to thank all my teachers, my mentors, and all who have made an influence in my life.

The financial support to this study by the Office of Naval Research and the National Science Foundation is acknowledged.

TABLE OF CONTENTS

	Page
LIST OF TABLES.....	viii
LIST OF FIGURES.....	ix
ABSTRACT.....	xiii
CHAPTER 1. INTRODUCTION.....	1
1.1. Laser Shock Peening.....	1
1.2. Problem Statement.....	2
1.3. Scope of this Research.....	2
1.4. Structure of this Thesis.....	3
CHAPTER 2. LITERATURE REVIEW.....	4
2.1. From High Energy Pulsed Laser to Shock Wave.....	4
2.2. Generation of Compressive Residual Stress by LSP.....	6
2.3. Effect of LSP to Components Mechanical Properties.....	8
2.3.1. Fatigue Performance.....	8
2.3.2. Resistance to Foreign Object Damage.....	9
2.3.3. Resistance to Stress Corrosion Cracking.....	10
2.4. Stability of the Compressive Residual Stress Generated by LSP.....	10
2.5. Residual Stress Relief Mechanisms.....	11
2.5.1. Residual Stress Relief and Dislocation Slip.....	11
2.5.2. Residual Stress Relief by Cyclic Loading.....	14
2.5.3. Residual Stress Relief by Thermal Annealing.....	14
2.6. Dislocations Stability.....	15

	Page
2.6.1. Dynamic Strain Aging	16
2.6.2. Dynamic Precipitation	17
2.7. Surface Processing at Elevated Temperatures.....	18
2.7.1. Warm Deep Rolling.....	18
2.7.2. Warm Shot Peening.....	18
2.8. Chapter Summary.....	19
CHAPTER 3. MATERIAL CHARACTERIZATION METHODS USED IN THIS THESIS	20
3.1. Micro-hardness Test.....	20
3.2. Surface Profile Measurement	20
3.3. TEM work	21
3.3.1. FIB H-Bar Method:	21
3.3.2. FIB Lift-out Method	22
3.4. Residual Stress Measurement.....	23
3.5. Fatigue Test.....	27
3.6. Chapter Summary.....	28
CHAPTER 4. WLSP OF ALUMINUM ALLOY 6061.....	29
4.1. Experiment and Characterization	29
4.1.1. Material	29
4.1.2. Warm Laser Shock Peening Experiments	30
4.1.3. Characterization:.....	31
4.2. Results and Discussion.....	32
4.2.1. Nanostructures Evolved Dynamically During WLSP	32
4.2.2. Surface Strength	33
4.2.3. Stability of the Compressive Residual Stress	34
4.2.4. Stability of the Dislocation Structure	36
4.2.5. Stability of Surface Strength at High Temperatures.....	37

	Page
4.2.6. Fatigue Performance.....	38
4.3. Chapter Summary.....	39
CHAPTER 5. WARM LASER SHOCK PEENING OF AISI 4140 STEEL	40
5.1. Experiments:.....	40
5.1.1. Material	40
5.1.2. Warm Laser Shock Peening Experiments	41
5.1.3. Characterization:.....	41
5.2. Results and Discussion.....	43
5.2.1. Process Conditions of Warm Laser Shock Peening	43
5.2.2. Microstructures Induced by DSA and DP.....	45
5.2.3. Nanostructures at Material Surface	53
5.2.4. Hardening effect by WLSP	54
5.2.5. Distribution of the Compressive Residual Stress	56
5.2.6. Thermal and Cyclic Stability of Surface Residual Stresses.....	57
5.2.7. Component Fatigue Performance after WLSP	59
5.3. Chapter Summary.....	61
CHAPTER 6. EFFECTS OF MICROSTRUCTURE TO CRACK PROPAGATION: A STUDY BY EXTENDED FINITE ELEMENT METHOD	62
6.1. Methods.....	63
6.2. Results and Discussion.....	68
6.2.1. the Stress Field Near the Crack Tip:.....	68
6.2.2. Effect of Volume Fraction of Nanoparticles on Fatigue Performance	69
6.2.3. Effect of Particle Size in a Constant Volume Fraction.....	71
6.3. Chapter Summary.....	73
CHAPTER 7. WARM LASER SHOCK PEENING OF COPPER	74
7.1. Simulation Method.....	74

	Page
7.1.1. Laser Induced Shock Pressure.....	75
7.1.2. Constitutive Modeling.....	76
7.1.3. Finite Element Model.....	79
7.2. Experimental Method.....	81
7.2.1. LSP at Elevated Temperatures.....	81
7.2.2. Residual Stress Measurement by X-ray Micro-diffraction System.....	82
7.3. Results and Discussion.....	82
7.3.1. Surface Deformation Profile.....	82
7.3.2. Surface Compressive Residual Stress.....	84
7.3.3. Surface Plastic Strain.....	87
7.3.4. In-depth Residual Stress and the Depth of Compressive Residual Stress.....	88
7.4. Chapter Summary.....	90
CHAPTER 8. CONCLUSION.....	92
LIST OF REFERENCES.....	94
VITA.....	99
PUBLICATIONS.....	100

LIST OF TABLES

Table	Page
Table 2.1 Shock Impedance of Common Materials.....	5
Table 4.1 Material Constant and Parameters Used for Residual Stress Measurement	31
Table 5.1 Material Constant and Parameters Used for Residual Stress Measurement	41
Table 6.1 Particle and Matrix Properties of Al ₂ O ₃ /6061 Al.....	67
Table 7.1 Peak Pressure at Different Laser Intensities	76
Table 7.2 Temperature Dependent Material Properties of Copper:.....	79
Table 7.3 Material Constant and Parameters Used for Residual Stress Measurement	81

LIST OF FIGURES

Figure	Page
Figure 1.1 Schematic Representation of the Laser Shock Peening Process.....	2
Figure 2.1 Time history of laser intensity temporal profile and the resulting plasma pressure temporal profile (Laser Intensity 4.1 GW/cm ² , Laser pulse width 5 ns, target material: copper, confining media: BK7 glass (Borosilicate crown glass), plasma peak pressure 7.8 GPa.)	6
Figure 2.2 Generation of compressive residual stress by LSP, adopted from Peyre [9], reuse with permission from Elsevier.....	7
Figure 2.3 Stress and strain behavior of the material during LSP	7
Figure 2.4 Surface plastic deformation as a function of the peak plasma pressure, adopted from Peyre [9], reuse with permission from Elsevier.....	8
Figure 2.5 Concept of stress intensity superposition: Compressive residual stress induced by LSP partially counterbalance the tensile stress.....	9
Figure 2.6 Residual stress relaxation of laser shock peened and deep rolled AISI 304 as a function of the test temperature after 2000 cyclic loading for a constant stress amplitude of 280 MPa, adopted from Nikitin [14], reuse with permission.....	11
Figure 2.7 Schematic Representation of the Residual Stress Generation and Relaxation by Atomic Structure	12
Figure 2.8 Schematic Representation of Atom Movement In Perfect Material Without Dislocation	13
Figure 2.9 Atoms Movement by the Movement of Edged dislocation, adopted from [22]	13
Figure 2.10 Schematic illustrating of dislocation pinning by solute atoms and precipitates, adopted from [25, 26].....	16
Figure 3.1 Automated Wyko NT3300 Major Components, adopted from Wyko NT3300 Manual	21
Figure 3.2 Schematic illustration of TEM sample preparation by the FIB H-bar method, re-drawn from [37] with permission from Elsevier	22
Figure 3.3 Schematic illustration of TEM sample preparation by the FIB lift-out method, re-drawn from [37] with permission from Elsevier	22

Figure	Page
Figure 3.4 D8-Discover GADDS micro-diffraction system from Bruker Inc, located in B2 of Grissom Hall of the School of Industrial Engineering, Purdue University	23
Figure 3.5 Schematic illustration of the parameters used in Bragg's law, adopted from Wikipedia [38]	23
Figure 3.6 Schematic representation of residual stress in crystalline materials and their impact to the diffraction patterns, adopted from Bruker internal report.....	25
Figure 3.7 a. The sample coordinate system; b. Five major components in a Bruker XRD system, and area detector, and X-ray generator, X-Ray optics (monochromator and collimator), goniometer and sample stage, and sample alignment and monitoring (laser/video) system, adopted from Bruker Internal Report	25
Figure 3.8 a. Snap shot of a single frame collected by Hi-star area detector; b. six 2θ peaks integrated from data in a. c. D-spacing versus $\sin^2\psi$ in a single ϕ direction	26
Figure 3.9 MTS servo-hydraulic fatigue testing system in the School of Industrial Engineering, Purdue University	28
Figure 4.1 Sample geometry, thickness 3.1 mm	30
Figure 4.2 TEM images of nanocrystals near top surfaces after RT-LSP (L) and WLSP (R).....	32
Figure 4.3 Dark field TEM images at different magnifications showing the dislocation arrangement and ultrafine precipitates after WLSP of AA6061.....	33
Figure 4.4 Hardness comparison between RT-LSP and WLSP for different laser intensities.....	34
Figure 4.5 Residual stress versus number of cyclic load for RT-LSP and WLSP at fatigue test stress magnitude 200 MPa.....	35
Figure 4.6 FWHM of 2θ versus number of cyclic loading for RT-LSP and WLSP	36
Figure 4.7 Hardness versus time of different samples at 170°C aging	37
Figure 4.8 S-N curve for as machined sample and laser peened sample	38
Figure 5.1 Surface residual stress for RT-LSP and WLSP (250°C) at different laser intensities and corresponding peak plasma pressure	44
Figure 5.2 Hardness at different temperature (laser intensity 4 GW/cm ²).....	45
Figure 5.3 Initial microstructure of quenched and tempered steel 4140 without peening showing (a) retained martensitic laths, and (b) Fe ₃ C cementite precipitates	46
Figure 5.4 TEM images of LSP sample (4 GW/cm ² room temperature) showing lamellar dislocation bands at different magnifications	47
Figure 5.5 TEM images of WLSP sample (4 GW/cm ² , 250°C) showing microstructures at different magnifications.....	48

Figure	Page
Figure 5.6 In-depth dislocation density comparison between LSP (Room temperature, 4 GW/cm ²) and WLSP (250°C, 4GW/cm ²)	49
Figure 5.7 Microstructure in room temperature LSP sample (Laser Intensity 4 GW/cm ²) (a) Bright field image showing the precipitates (arrows) near the subgrains.....	50
Figure 5.8 Microstructure in WLSP sample (Laser Intensity 4 GW/cm ² , Temperature 250°C) (a) dark field image taken from major diffraction spot showing the entanglement of dislocations and precipitates (b) diffraction pattern of the matrix and the diffraction spots (in-between the major spots, circled in the rings) from the precipitates (c) bright field image showing the lath precipitates and some globular precipitate (d) dark field image taken from diffraction spots associated with precipitates showing the globular precipitates generated by WLSP	52
Figure 5.9 TEM images showing nanostructures at the top surface after RT-LSP (left) and WLSP (right).....	53
Figure 5.10 Surface hardness at different laser intensities of RT-LSP and WLSP (250°C)	54
Figure 5.11 In-depth hardness comparison between RT-LSP and WLSP	55
Figure 5.12 In-depth residual stress comparison between RT-LSP and WLSP.....	57
Figure 5.13 (a) Residual stress relaxation after annealing at 350°C for different time of RT-LSP and WLSP samples; (b) Residual stress relaxation after cyclic loading at 1000 MPa maximal bending stress.	58
Figure 5.14 S-N curve for as machined 4140 steel sample and samples after RT-LSP and WLSP	60
Figure 6.1 a 2D Crack Representation in XFEM, adopted from [51].....	63
Figure 6.2 Flowchart for X-FEM integrated ABAQUS/Standard Toolkit, adopted from [51]	65
Figure 6.3 Model setup (the red arrow represents the crack) and mesh generated in ABAQUS... ..	67
Figure 6.4 Stress field near crack tip for models without (A) and with (B) nanoparticles	68
Figure 6.5 Stress concentration near the nanoparticles.....	69
Figure 6.6 Number of cycles versus crack length for different volume fractions.....	70
Figure 6.7 Comparison of da/dN for different volume fractions with the same particle size (100 nm).....	71
Figure 6.8 Number of cycles versus crack length for different particle sizes with the same volume fractions (10%).....	72
Figure 6.9 Comparison of crack propagation rate (da/dN) for different particle sizes with the same volume fractions (10%)	72

Figure	Page
Figure 7.1 Laser generated plasma pressure temporal profile (laser intensity = 4.1 GW/cm ² , pulsed laser duration at full width at half maximum (FWHM)).....	76
Figure 7.2 (a) Yield stress at different strain rates, atmosphere pressure, and temperature 300 K;(b) Yield stress at different temperatures, strain rate 1 s ⁻¹ , atmosphere pressure	78
Figure 7.3 Schematic view of model setup in ABAQUS.....	80
Figure 7.4 Comparison of surface contour after LSP between experiment and simulation (laser intensity 6.9 GW/cm ² , temperature 400 K)	82
Figure 7.5 Maximal displacement at different laser intensities and temperatures comparison between simulation and experiment (exp: experiment; sim: simulation)	84
Figure 7.6 Stress-strain curve of a single material point under LSP.....	85
Figure 7.7 Residual stress after LSP along beam center from simulation and experiment for different temperatures at laser intensity: 10.6 GW/cm ² , at 300 K.....	85
Figure 7.8 Peak compressive residual stress after LSP for different laser intensities and different temperatures from FEA model	86
Figure 7.9 Comparison of peak plastic strain in zz (depth) direction at different laser intensities and temperatures.....	87
Figure 7.10 In-depth residual stress (a) for different laser intensities at 300 K, and (b) for different temperature at laser intensity 10.6 GW/cm ²	89
Figure 7.11 Comparison of plastic affected depth after LSP at different laser intensities and temperatures.	90

ABSTRACT

Ye, Chang. Ph.D., Purdue University, August 2011. Investigation of the Stability of the Compressive Residual Stress Generated by Warm Laser Shock Peening. Major Professor: Gary Cheng.

Laser Shock Peening (LSP) has been successfully used to improve component fatigue performance by bringing beneficial compressive residual stress to material surface since the 1990s. However, it has been found that the compressive residual stress generated by room temperature LSP (RT-LSP) is not stable during cyclic loading. Thus, it is necessary to improve the stability of the compressive residual stress generated by RT-LSP.

In this study, Warm Laser Shock Peening (WLSP) is proposed as a potential approach to improve the stability of the compressive residual stress. WLSP is to laser peen a component that is being heated to elevated temperatures. As a thermomechanical treatment (TMT) technique, WLSP integrates the advantages of LSP, dynamic strain aging (DSA) and dynamic precipitation (DP). Through DSA, more uniform and high density dislocations are generated. Through DP, highly dense nanoscale precipitates are generated. Experimentally, WLSP has been evaluated by AISI 4140 steel in terms of the microstructure, residual stress stability and fatigue performance. To investigate the effect of the precipitate particles generated by WLSP to crack propagation, an extended finite element method (XFEM) model was employed. To investigate the effect of temperature to the residual stress distribution, WLSP simulation of copper, a pure metal not applicable to dynamic strain aging, was carried out by finite element model (FEM) and validated by experiments.

Through these studies, it has been found that: (1) WLSP can generate high density nanoscale precipitate particles in alloy materials applicable to dynamic strain aging and

precipitate hardening; (2) the highly dense precipitate particles generated by WLSP leads to higher material strength than RT-LSP; (3) the pinning force exerted by the precipitate particles to the dislocations leads to higher stability of the compressive residual stress; (4) the highly dense nanoscale precipitate particles generated by WLSP can dissipate the stress concentration near the crack tip and thus decrease the crack propagation speed and improve component fatigue performance.

PREVIEW

CHAPTER 1. INTRODUCTION

1.1. Laser Shock Peening

Laser shock peening (LSP) has been successfully used to improve metallic component fatigue performance for more than two decades [1]. In the current medium-confined LSP setup (Figure 1.1), a sacrificial coating and a transparent overlay are put on top of the target component. During LSP, the pulsed laser penetrates through the transparent overlay and irradiates on the sacrificial coating, the surface temperature of which increases rapidly [2]. When the temperature reaches certain point (around 10,000°C), plasma forms, which is confined between the target component and the confining medium. With the expansion of the high pressure plasma, shock wave propagates both in the target material and the confining media. In this way, the shock wave that goes into the material is stronger and lasts longer than free-expanding plasma in LSP without confining media. When the peak stress of the shock wave exceeds the Hugoniot elastic limit (HEL) of the material, plastic deformation occurs, which leads to the formation of compressive residual stress in component surface.

After LSP, the surface hardness of the metallic component increases, which is attributed to the work hardening induced by the high-strain rate deformation. Surface strength improvement combined with the presence of the compressive residual stress leads to fatigue performance improvement.

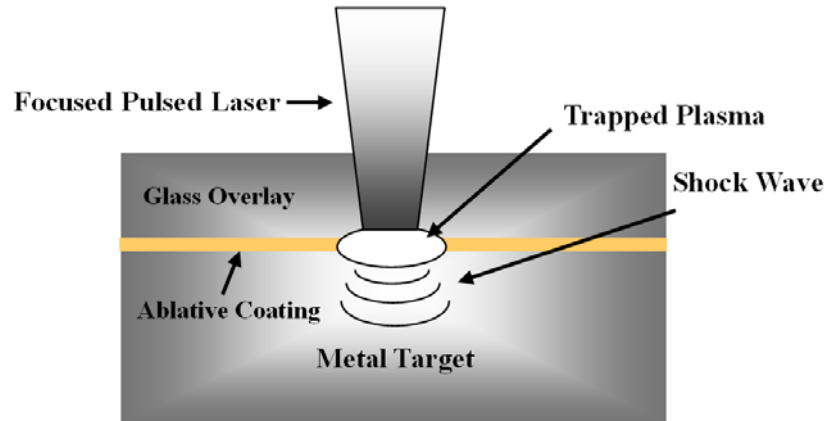


Figure 1.1 Schematic Representation of the Laser Shock Peening Process

1.2. Problem Statement

For effective fatigue life improvement by generating compressive residual stress by any surface processing technique (including LSP), two aspects are most important. Firstly, the magnitude of the compressive residual stress and secondly, the residual stress stability against cyclic loading, especially for cyclic loading at elevated temperatures.

The compressive residual stress magnitude generated by LSP is determined by the laser parameters and the material properties of the target component. The residual stresses generated by LSP are prone to decrease in magnitude during cyclic loading, especially at high loading temperatures [3]. If this happens, component fatigue performance cannot be effectively improved. Thus, it is very important to have stable compressive residual stresses.

1.3. Scope of this Research

Warm Laser Shock Peening (WLSP) is LSP while heating to target component to elevated temperatures, specifically the DSA temperature. WLSP integrates the advantages of LSP, dynamic strain aging (DSA) and dynamic precipitation (DP). By bringing compressive residual stress and nanostructures to component surface

simultaneously, it is expected that WLSP can stabilize the dislocations and thus improve the stability of the compressive residual stress. The aim of this research is to investigate the stability of the compressive residual stress generated by WLSP and to study how WLSP affect component mechanical properties.

In this study, aluminum alloys and carbon steels, both are applicable to DSA, were used to evaluate the WLSP process. To investigate how the microstructures generated by WLSP affect crack propagation behavior during cyclic loading, extended finite element method (XFEM) was used to model crack propagation under the influence of the precipitates generated by WLSP. To investigate the effect of temperature to residual stress generated by LSP, pure copper was used, since copper is not applicable to DSA or DP, its microstructure is relatively simple and it does not experience phase change during LSP at elevated temperatures.

1.4. Structure of this Thesis

This thesis is structured as follows. In Chapter two, a literature review is carried out on LSP and the related research work. Chapter three reviews the material characterization methods used in this study. Chapter four presents the WLSP work of aluminum alloy 6061. Chapter five presents the WLSP work on AISI 4140 steel. Chapter six presents an XFEM study of the crack propagation behavior under the influence of the microstructure generated by WLSP. Chapter seven presents the WLSP work of copper. Chapter eight draws the conclusion of this thesis.

CHAPTER 2. LITERATURE REVIEW

In Chapter one, the motivation of WLSP has been discussed and the scope of this research has been identified. In this chapter, a literature review is conducted on issues related to this research. This literature review includes, the generation of the compressive residual stress by LSP, how LSP affects component properties, the residual stress relief modes, the fundamental mechanisms of dynamic strain aging and dynamic precipitation, and the related work on high temperature surface processing in the literature.

2.1. From High Energy Pulsed Laser to Shock Wave

In LSP, the pulsed laser that is used to generate the high pressure plasma usually has high intensity (greater than 1 GW/cm²) and short duration (a few to 10s of nanoseconds). When a high power pulsed laser irradiates on to a material surface, the first atomic layer of the target material is vaporized into a high temperature (10,000°C) and high pressure (1-10 GPa) plasma. By performing a physical and mechanical study of the laser-induced plasma, Fabbro [4] described the relationship between the shock pressure $P(t)$ and plasma thickness $L(t)$ by:

$$\frac{dL(t)}{dt} = \frac{2P(t)}{Z} \quad \text{Eq. 2.1}$$

$$I(t) = P(t) \frac{dL(t)}{dt} + \frac{3}{2\alpha} \frac{d}{dt} [P(t)L(t)] \quad \text{Eq. 2.2}$$

Assume constant laser power density, I_0 , the scaling law for the pulse pressure can be estimated by:

$$P(\text{GPa}) = 0.01 \sqrt{\frac{\alpha}{2\alpha + 3}} \sqrt{Z(\text{g/cm}^2 \text{s})} \sqrt{I_0(\text{GW/cm}^2)} \quad \text{Eq. 2.3}$$

where P is the peak pressure and α (empirically value [4], typically, $\alpha=0.1\sim 0.2$) is the portion of absorbed energy contributed to the thermal energy of the plasma; Z is the reduced shock impedance between the material and the confining media, which is governed by Eq. 2.4:

$$\frac{2}{Z} = \frac{1}{Z_1} + \frac{1}{Z_2} \quad \text{Eq. 2.4}$$

where Z_1 and Z_2 are the shock impedance of the confining media and the target component respectively. The shock impedances of common materials are shown in Table 2.1. Figure 2.1 shows an example of laser power temporal profile and the generated plasma pressure temporal profile with BK7 glass (Borosilicate crown glass) as the confinement material.

Table 2.1 Shock Impedance of Common Materials

Material	Water	Aluminum	BK7 Glass	NiTi	Copper	Steel 4140	Stainless Steel 304
Shock Impedance ($10^6 \text{g}\cdot\text{cm}^{-2}\cdot\text{s}^{-1}$)	0.165 [5]	1.5*	1.44[6]	3.8*	4.18*	3.96*	3.94*

* Estimated by equation $Z=\rho\cdot D$ [7], where ρ is material density and D is shock wave propagation speed in material.

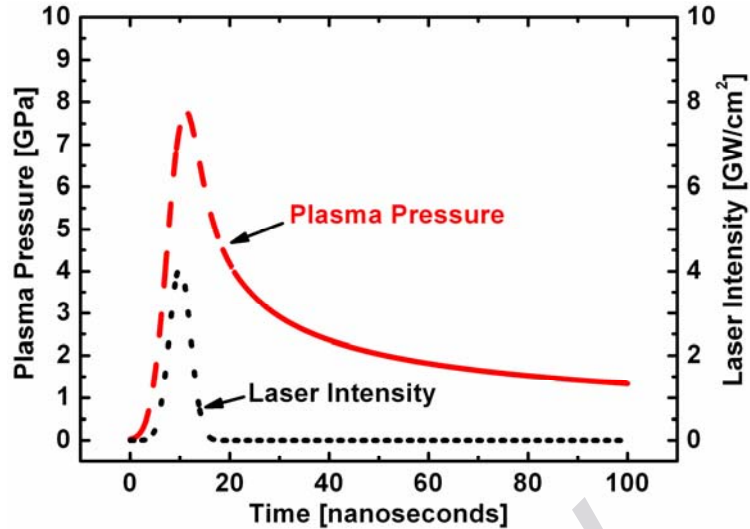


Figure 2.1 Time history of laser intensity temporal profile and the resulting plasma pressure temporal profile (Laser Intensity 4.1 GW/cm^2 , Laser pulse width 5 ns, target material: copper, confining media: BK7 glass (Borosilicate crown glass), plasma peak pressure 7.8 GPa.)

2.2. Generation of Compressive Residual Stress by LSP

When a high pressure is suddenly applied to a metallic target, the pressure is accumulated in the wave front, since it cannot disperse away within such a short time. Thus, a discontinuous jump of pressure, density, and internal energy is formed across the wave front [8]. In this way, the shock wave is formed.

When the shock wave that propagates into the material exceeds the dynamic yield stress of the material, plastic deformation occurs, which induces compressive residual stress in the material and change the near-surface microstructure and properties. The generation of residual stress consists of two steps [9, 10] : step (1) the rapid expansion creates sudden uniaxial compression (Figure 2.2a) on the irradiated area and dilation of the surface layer and step (2) the surrounding material reacts (Figure 2.2b) to the deformed area, generating a compressive stress field.

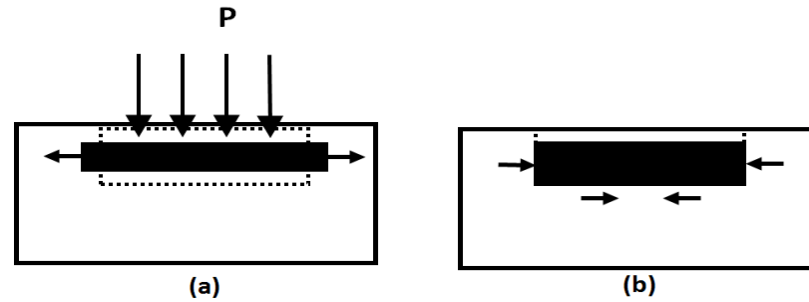


Figure 2.2 Generation of compressive residual stress by LSP, adopted from Peyre [9], reuse with permission from Elsevier

To evaluate the compressive residual stress, it is necessary to evaluate the plastic strain first. Figure 2.3 shows the material stress and strain behavior during LSP. In the loading process, the material stress increase linearly with the strain until the material yield point is reached. After that, the material work hardens and plastic strain occurs. In the unloading process, the stress-strain curve goes back to zero stress following a curve parallel to the elastic stress-strain line. At the end of the deformation process, some the elastic strain is recovered. The retained elastic strain corresponds to the residual stress after LSP. Ballard [11] analyzed the LSP process and proposed the relationship between the surface plastic strain and the peak plasma pressure as shown in Figure 2.4. The residual stress magnitude can be calculated by knowledge of the plastic strain, plastic affected depth and the material properties.

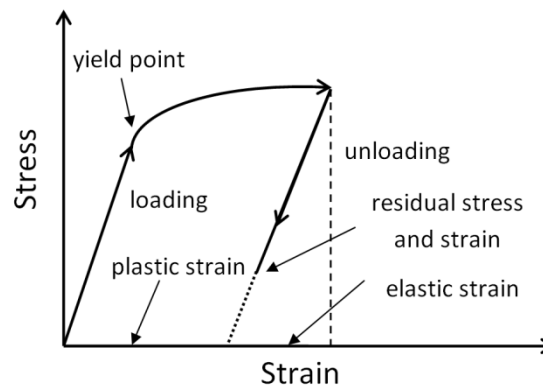


Figure 2.3 Stress and strain behavior of the material during LSP